Selim, M S, Shenashen, M A, Fathalla, N A, Elmarakbi, Ahmed and El-Safty, Sherif (2017) In Situ Fabrication of One-Dimensional-Based Lotus-Like Silicone/ ¥Al2O3 Nanocomposites for Marine Fouling Release Coatings. Chemistry Select, 24 (30). pp. 9691-9700. ISSN 9691-9700

Downloaded from: http://sure.sunderland.ac.uk/id/eprint/10942/

Usage guidelines

Please refer to the usage guidelines at http://sure.sunderland.ac.uk/policies.html or alternatively contact sure@sunderland.ac.uk.

In Situ Fabrication of One-Dimensional-Based Lotus-like Silicone/ϒ–Al_2O_3 Nanocomposites for Marine Fouling Release Coatings

Mohamed S. Selim,[a,b] Mohamed A. Shenashen,[a, b] Nesreen A. Fatthallah,[c] Ahmed Elmarakbi [d] and Sherif A. El-Safty [a,*]

Abstract: Prohibition on the utilization of organotins compounds in antifouling (AF), and Fouling release (FR) paints have attracted considerable ineptest as an environmentally friendly alternative. In this work, an ecofriendly series of lotus-like nano-structured organic-inorganic surfaces based on vinyl terminated polydimethylsiloxane (PDMS)/ϒ-Al_2O_3 nanorods composites were successfully modeled for the first time via in-situ technique. The tailored nanocomposites were cured via hydrosilation mechanism and applied for marine FR coatings. Incorporation of various concentrations of controlled 1D nanofillers was inevitable to study the structure property relationship. Mechanical tests, durability parameters, and the FR and biological inertness were assessed. The results confirmed that uniform distribution of the prepared ϒ-Al_2O_3 nanorods dramatically improved their water repellency, homogenous topology, self-cleaning and fouling repellency. With nanofiller insertion up to 0.5% nanofillers, a particular increase in the contact angle (CA), decrease in the surface free energy (SFE), and topological homogeneity was observed with improving phsico-mechanical, and durability against UV properties. The biological assessments indicated excellent inhibition and superior AF potential of the 0.5% nanofiller composite coatings. Our finding introduces attractive merits such as simplicity, ecofriendly, economic feasibility, and potential application in marine FR nano-coatings.

Introduction

Advances in nanomaterial science are accompanied by developing nanocomposite materials in terms of ecological and economic solutions for environmental problems. [1] Marine biofouling is a complex disaster that causes negative economic and ecological impacts in the marine environment and shipping industry. [2] Shipping is the prime facilitator of worldwide trade and economic growth as it represent larger than 90% of the international commerce. [3] Biofouling attachments on the ship hulls result in increased hydrodynamic weight and drag resistance which decrease service speed and loss of manoeuvrability. [4] As a result, fuel consumption increased up to 40% and the overall voyage cost can increase more than 77% with the emission of harmful compounds such as SO_x, NO_x and CO_2. [5] Traditional biocidal AF coatings can kill potential fouling organisms by leaching toxic compounds that also affect non-target species. [6] The wide-spread use of toxicants and their harmful effects on maritime communities followed by the universal prohibition by the international maritime organization (IMO) on the use of organo-tin compounds in 2001 have driven research toward non-leachant fouling release (FR) technology as an ecological and economic alternatives. [7, 8] Non-stick FR surfaces rely on a technology that acts by hindering the settlement of fouling organisms and weakening their adhesion strength. [9] Any adhered organisms can be facilely removed hydrodynamically ideally by simply bringing the ship to speed. [10] Silicone FR paints, particularly polydimethylsiloxane (PDMS), possess non-leachant properties, homogenous topology, environmental friendliness, stability in water, low free energy, optimum molecular mobility, water and fouling repellency, stability against heat and oxidation, and good adhesion on different substrate materials. [11] The superior properties of vinyl ended PDMS over hydroxyl ended PDMS reinforce their applications in self-cleaning FR technology. [12] The hierarchical nature and layer of waxes covering the lotus leaf produce a water repellent self-cleaning and ultra-hydrophobic surface called "lotus effect". [13] It is a common phenomenon in nature and is observed in lotus plants, rice plant, and butterfly wings that possess highly hydrophobic and self-cleaning surfaces. [13] Lotus-like based organic/inorganic hybrid nanocomposites with water contact angle (CA) larger than 150° and a considerably low roll-off angle represent a creative solution to design new nano-materials with improved or unusual features eco-friendly FR paints. [14] Lotus effect of a nano-coated surface is based on nano-micro binary structure and chemical functionality of the nanocomposite coatings. [15] Nano-filled PDMS elastomeric coatings have awarded great attention, owing to their unique properties possessed from hybridization of organic/inorganic hybrid compounds. [16] Progress in NP-based metal oxide paints is growing rapidly for the development of lotus-like surfaces for fouling inhibition. [17] The current work introduces for the first time an ecological series of self-cleaning FR coating models based on ϒ-Alumina (Al_2O_3) nanorod composites.

Nanomaterials with one-dimensional (1D) structures have gained considerable attention since the discovery of carbon nanotubes because of their abnormal electronic, mechanical and chemical features and their applications in biological fields. [18] ϒ-Al_2O_3, as a ceramic material, is perhaps the most important nanomaterial and can be applied in various fields as absorbent, catalyst carrier and reinforce of ceramic composites. [19] It possess many advantages such as low cost, extra-high surface area environmental friendliness, antibacterial activity, high strength, thermal and chemical stability, good electrical insulation and excellent antibacterial properties. [20] ϒ-Al_2O_3

---

[a] Dr. M. S. Selim, Dr. M. A. Shenashen, Prof. S. A. El-Safty; National Institute for Materials Science (NIMS), Research Center for Functional Materials, 1-2-1 Sengen, Tsukuba-shi, Ibaraki-ken, 305-0047, Japan. E-mail: sherif.elsafty@nims.go.jp
[b] Dr. M. S. Selim, Dr. M. A. Shenashen; Petroleum Application Department, Egyptian Petroleum Research Institute (EPRI), Nasr City 11727, Cairo (Egypt)
[c] Dr. N.A. Fatthallah; Processes Development Department, EPRI, Nasr City 11727, Cairo (Egypt).
[d] Prof. A. Elmarakbi; Automotive Composites Group, Faculty of Engineering and Advanced and Manufacturing, University of Sunderland, Sunderland SR6 0DD, UK.

Supporting information for this article is given via a link at the end of the document.

WILEY

single-crystalline nanorods with controlled size and morphology were prepared by thermal decomposition of boehmite (γ-AlOOH) precursor that was synthesized by solvothermal technique. [21] Modelling superhydrophobic surfaces based on γ-Al_2O_3 nanorods array depend on the combination of both rough and hierarchical structures as well as low SFE. [22, 23] These outstanding features prompted our research to prepare in-situ silicone enriched γ-Al_2O_3 nanorods structured composites with novel FR terminology resulting from synergetic interaction of micro-nano binary structure. The volume fraction, nanofiller type, morphology, percentage, and interfacial properties of individual constituents are the main factors in determining PDMS composite behaviour. [24] This work is concentrated on applying stable thin-film, eco-friendly, superhydrophobic, cost-effective and non-stick self-cleaning FR nanocomposite surface with lotus-like properties via in-situ method. Well dispersion of nanofillers can greatly enhance surface properties such as CA, SEF and topological homogeneity. [25] Quantitative measurements were also used to be applied to investigate the physicomechanical properties as well as UV and thermal stability. Biodegradability measurements and turbidimetric prediction has been used to trace concentration and mass of bacterial suspensions. [26] Novel lotus-like in-situ silicone/single crystal Al_2O_3 nanorods composites based on surface hierarchical nano-roughening array were applied for self-cleaning FR coating following physical anti-adhesion mechanism. Ecological and economic impacts, long term durability, ease of fabrication, high FR performance and stability against wide range of PH values are the prime merits introduced in this novel work.

Results and Discussion

Shape and diameter size control of the as-synthesized γ-Al_2O_3 nanorods

It is widely accepted that controlling the experimental factors could affect the particle size, shape and stability of the nanomaterials. The preparation technique of γ-AlOOH nanorods is very sensitive to pH variations of the solution. Changing the pH values can greatly affect the particle morphology. In the hydrothermal technique for the preparation of γ–AlOOH, varying the pH from 4 to 10 may result in preparation of the 1D nanorods and nanorods and 2D nano-flakes. Changing pH values to lower values (pH < 4), no precipitates can be obtained in hydrothermal reaction. It was reported that, synthesis of γ-AlOOH particles at pH of 5 and 200 °C, can exhibit whole nanorods morphology with an average diameter of 20 nm and lengths of 150-200 nm. [27] This is due to the characteristic structure of γ–AlOOH, which has a lamellar structure of linked octahedral AlO6 units to form an infinite plane perpendicular to the [010] direction. [27] The lamellar structure is sustained by hydrogen bonding of the OH groups. Then the OH groups covered the lamellar surfaces, in which the oxygen lone pairs are directed outwards. H+ generated in the reaction solution under acidic conditions can combine with lone pair of oxygen in the OH groups to give aqua ligands. [19] This result in destroying the γ–AlOOH layers. Subsequently, the separated curl to form 1D nanostructure via the scrolling-growth route. [28] Also, changing calcination temperatures of the prepared γ-AlOOH nanorods from 400 ºC to 1300 ºC, can greatly affect the product. It was reported that calcination at temperature 500-1200 can transform the sample to γ-Al_2O_3. However higher temperatures can yield hybrid phases with θ-Al_2O_3 and α-Al_2O_3.

It was reported that calcination at 500 ºC result in producing γ-Al_2O_3 similar in size and morphology to those of the γ-AlOOH precursor. The synthetic technique of the preparation of γ-Al_2O_3 nanorods were successfully achieved with controlled size and shape as indicated in Scheme 1. Great influence of the particle size and morphology is necessary for lotus-like FR coating with high self-cleaning properties. FTIR spectrum of the as-synthesized γ-Al_2O_3 nanorods revealed that the stronger broadening band observed at 3476 cm^{-1} is due to the hydrogen bond between the various hydroxyl groups in the prepared sample. The bands observed at 803 cm^{-1} and from 591 cm^{-1} correspond to Al-O vibrations of v-AlO_4 and v-AlO_6, respectively (see Supporting Information, Figure S1).

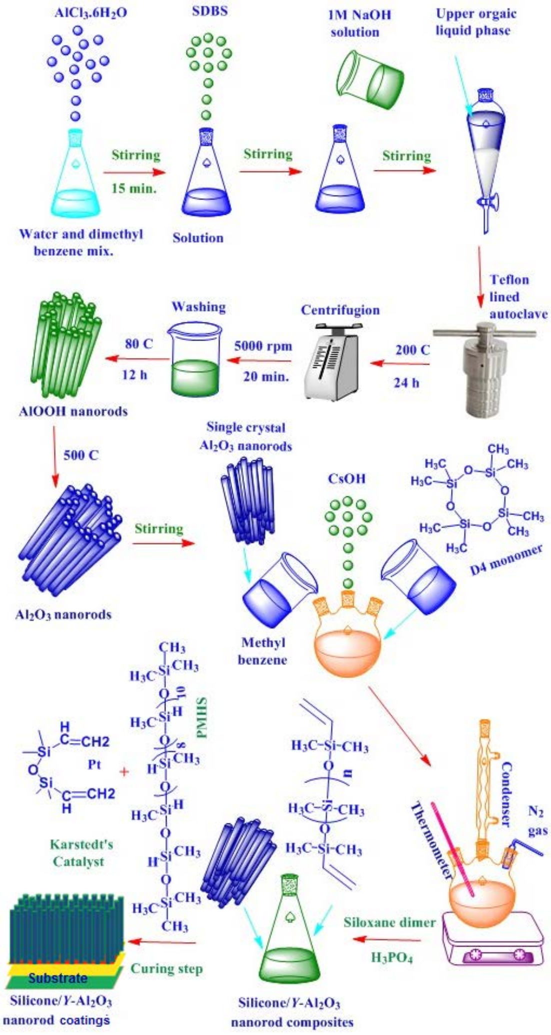

Scheme 1. Synthesis of single crystal γ-Al_2O_3 nanorods via hydrothermal and heating techniques as well as an in-situ synthesis of silicone/single crystal γ-Al_2O_3 nanorod composites.

The XRD spectrum of the as-synthesized Ƴ-AlOOH nanorods suggested that they were orthorhombic phase and the values are compatible with the literature values of (JCPDS No. 21-1307). The peaks observed at 2θ = 14.67°, 28.31°, 39.14°, 46.40°, 49.52°, 52.73°, 56.45, 60.6, 65.4, 66.7 and 68.74° were the {020}, {120}, {031}, {131}, {051}, {220}, {151}, {080}, {231}, {002} and {171} interplanar reflections of nanorod crystal system, respectively. No impurity peak was observed, which confirmed the high purity of the prepared γ–AlOOH. After calcination at 500 ºC, the prepared *γ-Al_2O_3 nanorods* were confirmed by XRD through comparing with JCPDS No. 29-63. as indicated in (Figure 1). The peaks observed at 2θ = 37.67°, 47.31°, 59.14°, 76.40° were the {311}, {400}, {511} and {440} interplanar reflections of nanorods crystal system, respectively. The spectrum revealed the highest intensity of the {400} peak than the other peaks, indicating that this planes is the preferential growth direction of γ -Al_2O_3.

Debye–Scherer equation (1) was utilized to calculate the average diameter (D) of the prepared γ -Al_2O_3 nanorods, [29] and the range was within the mean.

$$D = \frac{K \times \lambda}{FWHM \times cos(\theta)}. \qquad (1)$$

where K represents the Scherrer constant for nanorods morphology; while θ, FWHM and ƛ represent Bragg's angle, full-width-at-half-maximum of the spectrum, radiation wavelength, respectively. Crystal facet {400} plane was observed to be the highest intensity (Figure 1).

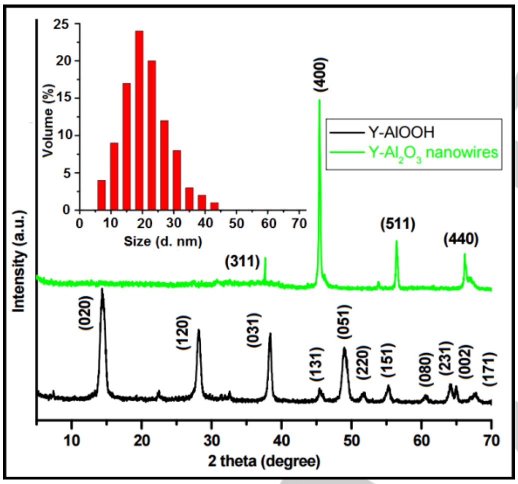

Figure 1: XRD pattern of the prepared γ-Al_2O_3 nanorods and inside DLS of the as-synthesized nanorods.

HRTEM images of the as-synthesized single crystal γ-Al_2O_3 nanorods were indicated in Figure 2, where figure 2 (A-D) indicated that the preparation of uniform size, single crystal whole nanorods with 20 nm average diameter. Results confirmed the nanorod structure of the prepared NPs without impurities. Figure 2E exhibit single crystal nanorods and clear lattice fringes with d spacing of 0.25 corresponding to the separation between the neighboring lattices. The inset of Figure 2F presents the selected area electron diffraction (SAED) pattern taken from a single nanorod, which can be indexed as single-crystalline structural γ-Al_2O_3. The crystal plains {400}, {511}, and {440} were indexed according to the pattern from SAED results, which agreed with those obtained from XRD.

Also the preparation of γ-Al_2O_3 nanorods was confirmed via EDXA spectrum (Figure 2G). Elemental mapping of the as-synthesized single crystal γ-Al_2O_3 nanorods demonstrated their purity with only aluminum and oxygen being detected. EDX analysis provides average atom percentage of O and Al is 62.04 and 37.96, respectively. Homogenous diameter size of the prepared γ-Al_2O_3 with nanorods morphology and single crystal structure were observed via the FESEM images (Figure 2H and I).

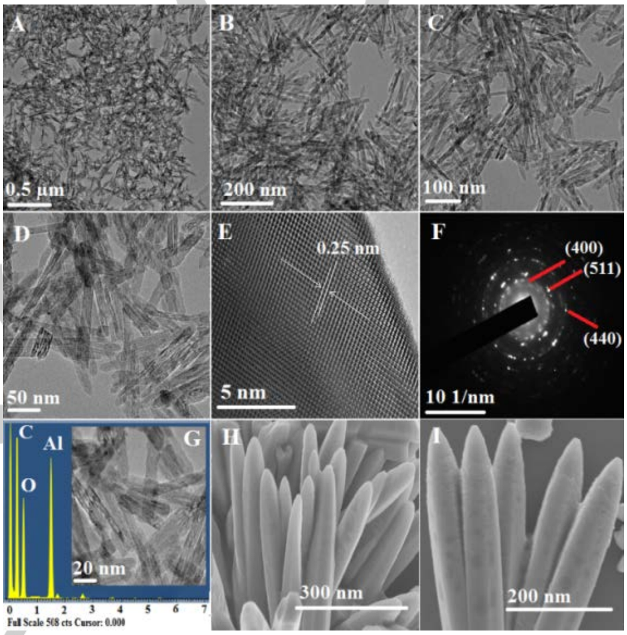

Figure 2: (A)–(D) are the HRTEM captures of the as-synthesized γ-Al_2O_3 nanorods at different magnification powers; (E) corresponding crystal lattice of the prepared γ-Al_2O_3 nanorods; (F) represent SAED patterns of the prepared γ-Al_2O_3 nanorods; (G) corresponding EDX pictures of the prepared γ-Al_2O_3 nanorods; (H) and (I) corresponding to the FESEM images of the as-synthesized γ-Al_2O_3 nanorods.

XPS measurements were performed to investigate the chemical states of the prepared single crystal γ-Al_2O_3 nanorods as shown in Figure 3 (A–D). Wide scan spectrum indicated the presence of Al, O and C elements and that the synthesized samples are pure Al_2O_3 with no impurities as shown in Figure 3 (A). The association of Al with oxygen in the completely oxidized state was confirmed from the binding energy of Al 2p observed at 73.93eV peak (Figure 3B). Two sub-peaks of O1s core level peak with a shoulder shape were observed with one at 531.03 eV attributed to the O^{2-} ions in the wurtzite structure surrounded by Al atoms with a full complement of nearest neighbor O^{2-} ions as indicated in Figure 3(C). A highly electronegative environment with charged O^{2-} ions in the geometry of a Wurtzite structure is the reason for the highly electropositive Al^{3+} which is in agreement with the chemical states of Al and O atoms obtained. Figure 3D indicated the presence of strong C1s peaks in the sample is from the carbon tape utilized for XPS characterization.

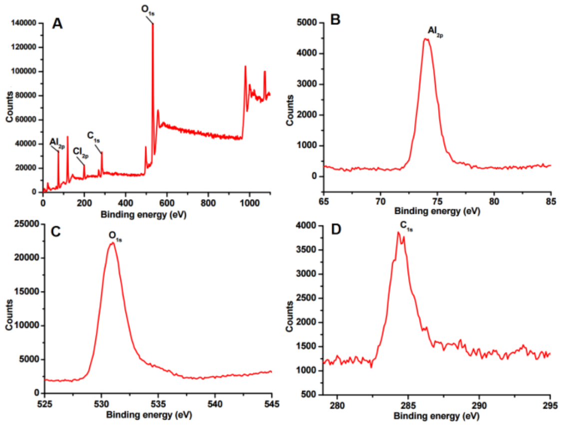

Figure 3: XPS measurements of single crystal γ-Al_2O_3 nanorods; (A) wide scan spectra (B) core level spectra for Al_{2p} (C) core level O_{1s} spectra and (D) C_{1s} spectra.

Fabrication of unfilled and γ-Al_2O_3 nanorods–silicone nanocomposites and NP dispersion

Advantages of high MW of vinyl ended PDMS and catalytic addition of Si–H bonding in crosslinking reaction awarded great interest recently especially their applications in self-cleaning coatings. Their modeled composites and nanosurfaces possess several surfaces, physical and mechanical advantages which enabled their applications in marine FR coatings. It was reported that Young's modulus and tensile strength elongation at break were improved with high MW of PDMS as compared with the low MW analogs. [30] It has been also demonstrated that in situ nanocomposites impart better properties than ex situ nanocomposites. [31]

However, there is no report on the in-situ PDMS/γ-Al_2O_3 nanorod composites where polymerization is carried out with the monomer in presence of nanofiller. Various concentrations of single crystal γ-Al_2O_3 nanorods were sonicated in the utilized OMCTS "octamethylcyclotetrasiloxane" monomer to prepare the as-synthesized nanocomposites. This research makes the first attempt to synthesis in-situ PDMS/γ-Al_2O_3 nanorods and analyzes the structure-property relationship of the tailored nanocomposites and their performance in maritime navigation. Superhydrohobic surfaces were produced with hierarchical roughness and low SFE. The low-surface energy {400} orientation of γ-Al_2O_3 nanorods stabilized and enhanced the lotus effect. γ-Al_2O_3 nanorods exhibit remarkable properties owing to their ultra-water repellent and antibacterial properties even at very small percentage. Lotus effect of the prepared γ-Al_2O_3 nanorods exhibit high performance via control of NP morphology and average diameter. This approach was used to develop a novel γ-Al_2O_3 nanorods enriched with PDMS composites with loading different nanofiller percentages that can hinder fouling settlement and enhance the surface inactivity. HRTEM images of the prepared PDMS/γ-Al_2O_3 nanorod composites were investigated (Figure 4 A, B, C and D) where γ-Al_2O_3 were reflected as distributed dark particles and surrounded by uniformly bright silicone background. TEM pictures of the prepared γ-Al_2O_3 nanorods/PDMS composites (0.5% nanofiller concentration) showed good distribution without any aggregation or particle clustering properties (Figure 4A and B). The well dispersion behavior of γ-Al_2O_3 nanorods in silicone composites considerably enhanced the physicochemical, superhydrophobic, topological homogeneity, self-cleaning and fouling inhibition characteristics. On contrarily, NPs clustering take place at high concentrations of nanofiller (1% γ-Al_2O_3 nanorods) (Figure 4 C and D). Clustering of NPs result in reduced topological homogeneity, superhydrophobicity and self-cleaning behaviour, thereby facilitating fouling settlements. Also, FESEM of the as-synthesized silicone film indicated the smooth topology obtained for unfilled sample (Figure 4E). While well distributed in-situ silicone/Υ-Al_2O_3 nanorods composites approved the performance of nanorods in improving the rough topological homogeneity which is an essential parameter for lotus-like FR behaviour (Figure 4F and G). FESEM images (top-view) of PDMS/Υ-Al_2O_3 nanorod composite surfaces were indicated in Figure S2 ((A and B) in the Supporting Information) and inside are magnified SEM image showing the hierarchical nature and integrity of the nanorod arrays in the nano-coating.

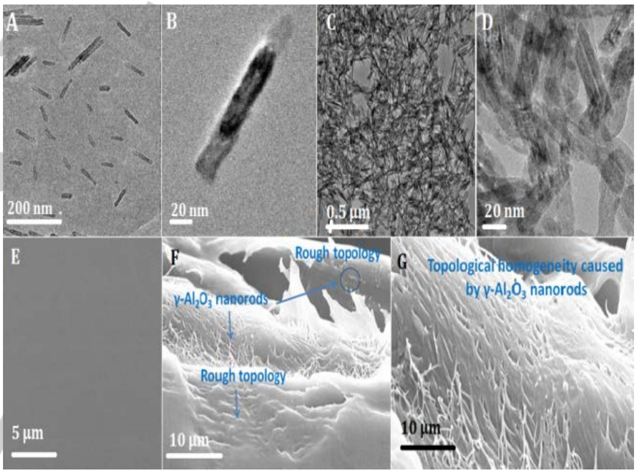

Figure 4: (A) and (B) corresponding TEM images of the as-synthesized well-dispersed PDMS/ Υ-Al_2O_3 nanorod composites (0.5% nanofillers) at different magnifications; (C) and (D) are TEM images of the prepared PDMS/ Υ-Al_2O_3 nanorod composites at high filling concentration that cause agglomerations (1% nanofillers) at different magnifications; (E) corresponding to FESEM of the prepared unfilled PDMS surface and (F) and (G) are FESEM of the as-synthesized PDMS/Υ-Al_2O_3 nanorod composites at different magnifications which clarify the superhydrophobic nature caused by the hierarchical rough topology of Υ-Al_2O_3 nanorods.

Superhydrophobic surface of in-situ PDMS/γ-Al_2O_3 nanorod composites

For designing lotus-like silicone self-cleaning coatings, superhydrophobicity surface properties are controlled by controlling nanofiller type, shape, size and distribution properties. Static CA measurements were determined for the prepared virgin and in-situ filled PDMS/γ-Al_2O_3 nanorods composites before and after immersion in water and also after drying (Figure 5A). The results indicated that for cured unfilled PDMS, hydrophobic properties were observed with static CA of 108°±2° values. This increased CA compared with other commercial silicone resins, such as Sylgard 184 (104°) and RTV11 (101°) was influenced by the high MW nature of the as-synthesized PDMS.

With varying nanofiller concentrations, the surface rough and hierarchical topology and low SFE non-wettability characteristics of the designed silicone/γ-Al_2O_3 nanorods composites change considerably. [32] This hierarchical roughness promotes the trapping of air between the water droplet and surface, thus preventing water from penetrating into the surface. [33] Modulating the surface roughness combined with chemical modifications is generally an effective way to achieve a superhydrophobicity surface with a large contact angle. [34]

Static CA measurements were found to increase gradually with nanofiller insertion up to 0.5% nanofillers (169° ± 1°) and decrease gain at high nanofiller loadings for 0.7% and 1% (143° ± 2° and 122° ± 2°; respectively). These measurements confirmed the lotus-like structure awarded from the well-distribution of γ-Al_2O_3 nanorods (0.5% nanofillers) and the absence of particle clustering in the tailored nanocomposites. Increasing the NP surface area to the volume ratio and enhancing the interfacial chemical bonding between polymeric matrix and NPs can greatly improve the surface topological homogeneity and lotus effect performance. On contrarily, higher γ-Al_2O_3 concentrations in the PDMS exhibit gradual reduction in water repellency with WCA of 139± 2° and 124° ± 2°(for 0.7% and 1% nanofillers) as illustrated in figure 5A. These results are due to the aggregation and particle clustering of γ-Al_2O_3 nanofillers which weaken the polymer-NP bond strength between the clustered particles, thereby reducing the NP surface area to volume ratio. This result in topological heterogeneity and reduction in surface self-cleaning and fouling resistance behaviour on the aggregated composite films. After immersion in DI water for 7 days, lower CAs were observed than un-immersed samples and restore their water-repellency characteristics after and this reflects the renewable nature of the tailored surfaces and nanofilms. SFE calculations (Figure 5B) were carried out for designed virgin and in-situ filled silicone/γ-Al_2O_3 nanorods composites via geometric mean terminology. The value of unfilled high MW PDMS exhibit 21.46 mN/m which is lower than the results reported for FR coatings such as sylgard 184. [8] At lower nanofiller concentrations, γ_s^{total} decreased gradually till 0.5% to 10.03 mN/m. The minimum reported surface tension at 0.5% resulted from the insertion of well-distributed γ-Al_2O_3 nanorods inside the polymer matrix which can achieve surface inertness toward fouling settlements. On contrarily, high nanofiller concentrations can gradually increase γ_s^{total} up to 17.03 mN/m for 1% γ-Al_2O_3 nano-fillers which can be attributed to the reduction in topological homogeneity caused by NPs agglomerations and aggregations.

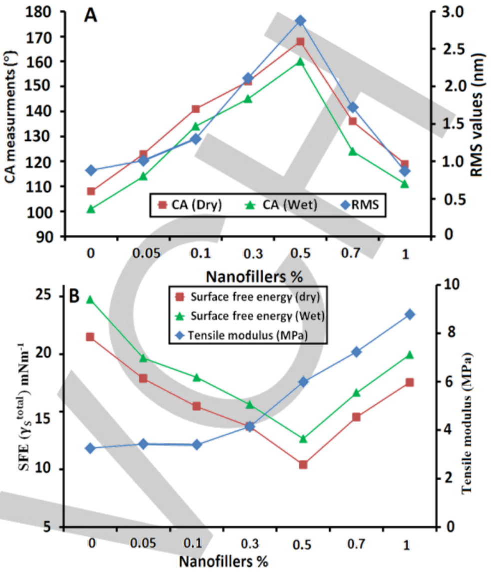

Figure 5: (a) WCA determinations of the as-synthesized virgin and measurements of the prepared unfilled and PDMS/γ-Al_2O_3 nanorod composites before and after immersion (Error bars represent ±2 standard deviations based on three determinations) and inside the RMS values obtained from AFM measurements (Error bars represent ±0.01 standard deviations from three replications); (b) SFE for the virgin and PDMS/γ-Al_2O_3 nanorod composites before and after immersion in distilled water for 7 days (Error bars represent ±0.2 standard deviations based on three determinations) and inside modulus of elasticity of the γ-Al_2O_3 nanorod/silicone nanocomposites (Error bars represent ±0.1 standard deviations from three replications).

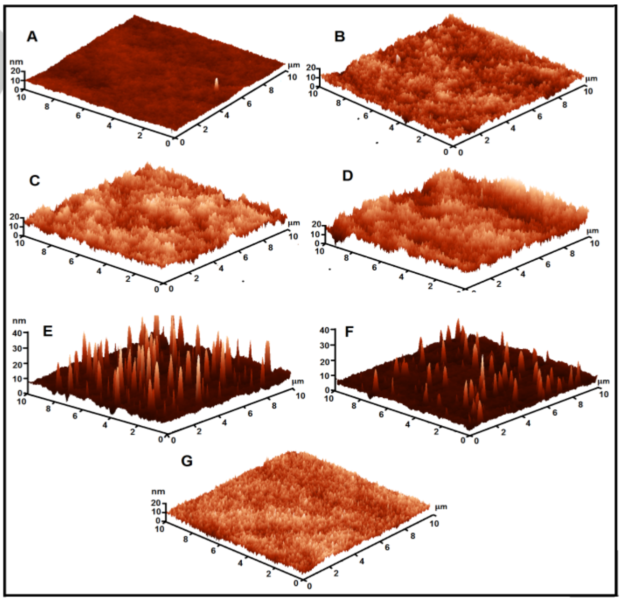

Figure 6: Three-dimensional AFM surface images of the coating films; (a) virgin cured PDMS surface; (b) PDMS/ γ-Al_2O_3 nanorod composites (0.05% nanofillers); (c) PDMS/ γ-Al_2O_3 nanorod composites (0.1% nanofillers); (d) PDMS/ γ-Al_2O_3 nanorod composites (0.3% nanofillers); (e) PDMS/ γ-Al_2O_3 nanorod composites (0.5% nanofillers); (f) PDMS/ γ-Al_2O_3 nanorod composites (0.7% nanofillers); (f) PDMS/ γ-Al_2O_3 nanorod composites (0.7% nanofillers); (G) PDMS/ γ-Al_2O_3 nanorod composites (1% nanofillers).

These results are confirmed by AFM test (Figure 6) which can characterize the surface topology and morphology of the tailored nanocomposites. Unfilled PDMS film (Figure 6A) reveals a uniform, featureless and smooth surface where the RMS of the virgin film is 0.874 nm. With increasing the nanofiller concentrations (0.05%, 0.1% and 0.3%), the topological homogeneity increase gradually as indicated in Figure 6 (B, C and D). For well-distribution of nanofillers in the in-situ PDMS/ γ-Al_2O_3 nanorods (0.5% nanofillers), it is clear that surface morphology become much rougher with RMS of 2.93 nm due to its hierarchical surface morphology (Figure 6E). Owing to the higher RMS value of the well-distributed hybrid nanocomposite film, the as-synthesized surface shows much higher WCA. For high nanofiller concentrations (0.7% and 1% of γ-Al_2O_3 nanorods as indicated in Figure 6 (E and F) in the in-situ prepared nanocomposites, it is clear that surface morphology exhibit gradual decrease in surface homogenity with RMS value of 0.887 nm (for 1% nanofillers) due to its agglomerations and particle clustering that reduce the surface topological homogeneity and reduce WCA. Thus, an ultra-smooth topology and slippery surface was fabricated which weaken the fouling bonds of attachments to the surface (Scheme 2). These results go in agreement with those obtained from CA and SEF measurements and approve the superior FR lotus-like structure of good-distributed 0.5% γ-Al_2O_3 nanorods concentration. While 1% nanofiller loadings exerted minimum FR self-cleaning properties among the filled nanocomposites because of the particle clustering. The highest WCA, minimum SFE and the maximum topological homogeneity at 0.5% resulted from inserting well dispersed γ-Al_2O_3 nanorods inside the PDMS resin which afford surface inertness against fouling.

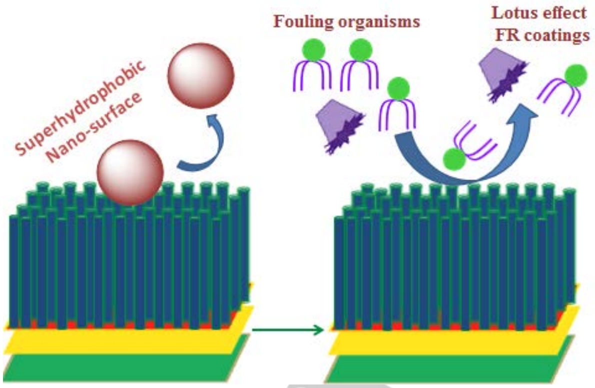

Scheme 2: Superhydrophobic surface of PDMS/single crystal γ-Al_2O_3 nanorod FR composites behaviour and their failure adhesion mechanism.

The chemical bonding between the NPs and polymer matrix and the mechanical features of the tailored nanocomposites were evaluated by tensile modulus test (Figure 5B). The test exhibits approximately no change, the elasticity remains constant, with γ-Al_2O_3 nanorods loadings up to 0.5%, because of the well-dispersion of NPs inside the polymer matrix. However, tensile modulus increased with high filling ratio of about 1% which reflected the stiffness and brittlness of nanocomposites obtained from aggregation and particle clustering. The NPs agglomerations decreased the chemical bonding with the PDMS resin. As a result, single crystal nature of γ-Al_2O_3 fillers with nanorod morphology, particle size 20 nm enclosed by {400} lattice plane are major parameters controlling the chemical activity and enhancing surface self-cleaning and fouling resistance ability.

Comparable studies of the tailored γ-Al_2O_3 nanorods /silicone nanocomposite models

Single crystal γ-Al_2O_3 nanorods exposed with {400} facets were easily synthesized and controlled in shape and morphology for developing novel series of lotus-like superhydrophobic, self-cleaning FR Nano surfaces for maritime navigation. Lotus effect self-cleaning properties are greatly affected by enrichment with the controlled γ-Al_2O_3 nanorods shape and morphology. As a result CA was greatly enhanced and surface tension was reduced for the designed nanocomposites as compared with virgin surfaces. WCA and SFE are greatly influenced by well-distribution of γ-Al_2O_3 nanofiller concentrations that was approved to be higher for 0.5% nanorods percentages than other nanocomposite concentrations. Both the roughened structure and the low SFE of the nanocomposite endue the γ-Al_2O_3 surface with the outstanding superhydrophobic property. These comparative studies reflected the promising features introduced by these newly developed well-dispersed nanocomposites as compared with other commercial and newly developed FR surfaces and nanocoatings as follow:

- Two commercial FR models, namely, Sylgard 184 (Hydrosilation cured silicone surface) and RTV11 (condensation cured silicone surface) were included in the comparison. [12]
- A developed Sylgard 184/-speolite multiwall carbon nanotube (MWCNT) nano-coating system. [35]
- Tailored designed easy cleaning hydrosilation cured PDMS/Cu_2O nano-cubes composites (with good distributed 0.1% cubic Cu_2O nanofiller loadings). [8]
- Modeled self-cleaning PDMS/spherical Ag nanocomposites (with well-dispersed 0.1% nanofiller loadings). [16]
- Fabricated RTV/spherical ZnO (CA of 132.5° and RTV/ZnO–SiO_2 (162.7°). [36]

All these nanocomposites were applied in previous studies for water repellent, self-cleaning and FR coatings. [37] Comparison of our developed in-situ silicone/single crystal γ-Al_2O_3 nanorods with these commercial and developed systems followed Wynne et al hypothesis that compared Sylgard 184 and RTV11 based on CA and SFE measurements. [12] The excellent-dispersed 0.5% single crystal γ-Al_2O_3 nanorods concentration with enhanced NP's surface area and interfacial chemical bonding between the matrix and nanofillers affording desirable rough homogenous topology, lotus effect and slippery FR surface with maximum performance than the aggregated 5% concentration (Figure 5 (A and B)). The designed single crystal γ-Al_2O_3 nanorods/silicone composite structures with the most effective concentration (0.5% nanofiller loadings) achieved the optimum self-cleaning characteristic, the most homogeneous surface rough topology and the minimum SFE among the tailored nanocoatings utilized in the comparable study (Figure 7). Thus the most profound FR and self-cleaning performance was referred to the current in-situ silicone/single crystal γ-Al_2O_3 nanorod composites (0.5% nanofillers). This superhydrobicity induced by fabrication of a rough surface with low SFE materials. The ecofriendly trend of the as-synthesized in-situ silicone/single crystal γ-Al_2O_3 nanocomposites was mainly due to the enrichment by single crystal γ-Al_2O_3 nanorods exposed with {400} crystal plane that minimize their SFE as a result of enhanced chemical bonding in the coating nanocomposites. The results approved the low SFE and higher CA of the tailored in-situ silicone/single crystal γ-Al_2O_3 nanorods (20 nm average diameter) composites essentially associated with a high density {400} crystal plane, is more prominent than 90 nm lower density{100} crystal plane along the cubic Cu_2O NP domains. Also {400} facets of γ-Al_2O_3 nanorods reduce the SFE and improve the lotus effect, self-cleaning performance and FR performance more than {111} crystal plane in silver composites. Also the reported CA values of RTV/ZnO (CA of 132.5° and RTV/ZnO–SiO_2 (162.7°) were mentioned in the comparison. The maximum WCA (169°±1°) and reduced SFE (10.03 mJ m^{-2}) as well as the homogenous rough topology obtained from AFM reflected the superior FR and lotus effect properties of the well-dispersed PDMS/ single crystal γ-Al_2O_3 nanorods (0.5% nanofillers).

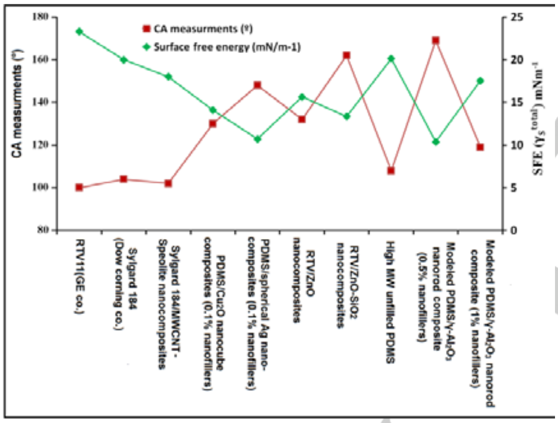

Figure 7: Comparison of the as-synthesized silicone/γ-Al_2O_3 nanorod composites and other commercial developed and sounded FR surfaces.

Stability behaviour

- **Stability against different pH solutions**

Via submersion in different pH solution values (4, 6, 7, and 9-10), the stability of the tailored superhydrophobic nano-surfaces were assessed after immersion. These values were used considering that acid rains, tap water, DI water and washing liquor exhibit PH values of 4, 6, 7, 9-10.5, respectively. WCA determination was carried out after submersion in pH buffer solution for 10 days; results illustrated a slight decrease in the determined WCAs where all the specimens are in their water-repellent characteristics. Nevertheless, the decrease after immersion was more pronounced for tap water solutions than in other solutions because of ionic contamination. This effect can restore the surface water repellency and static WCA properties after drying. Thus, this behavior reduced the transition from superhydrophobic Cassie to superhydrophobic Wenzel state, which may be attributed to a slight elimination of the coated film. The results reflected that the prepared nanocomposite coatings exhibited excellent stability against a wide range of pH solutions, specifically the well-distributed PDMS/ γ-Al_2O_3 nanorod composites (0.5% fillers loadings) because of the extra-high bonding strength between the NPs and the polymer matrix as well as the improved surface area.

- **Thermal and UV stability**

The stability of surface properties against UV exposure is a vital consideration in studying superhydrophobic self-cleaning nanocomposites. [26, 38] An accelerated aging test was conducted according to ASTM G154 standard to investigate the stability of the superhydrophobic surface under UV irradiation. Each assessment performed by QUV device contained two parts of UV rayon and condensation (RH%=65±3%). Static WCA measurements illustrated that, the water-repellent surface remained stable after four test cycles. These results proved the high resistance of the as-synthesized single crystal γ-Al_2O_3 nanorods composites against UV and humidity (Figure 8A).

Investigating the coating thermal stability is crucial which was carried out by heating the coated specimens up to 150 °C for different times. The tailored nanocoatings manifested excellent surface stability after heat exposure through placing in an oven for one month (Figure 8B). A Lotus-like surface with static WCA of 169°±1° (for 0.5% nanofillers), therefore the prepared nano-surface retained their self-cleaning and superhydrophobic characteristics and approve high stability against thermal contact.

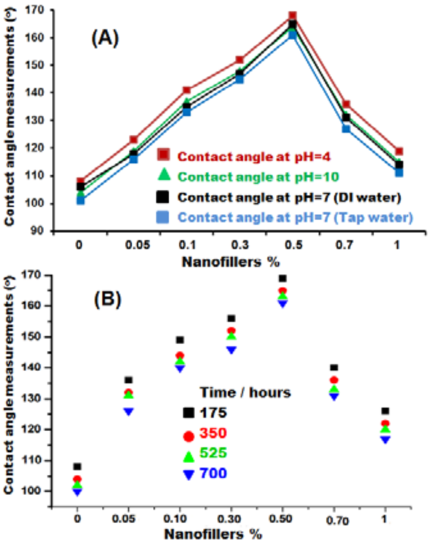

Figure 8: (a) Static WCA determinations of the as-synthesized virgin and PDMS/γ-Al_2O_3 nanorod composites as a function of immersion time in different pH solutions for 10 days. (Error bars represent ±1 standard deviations based on three determinations); (b) Thermal stability of the as-synthesized virgin and γ-Al_2O_3 nanorods filled PDMS nanocomposites verses times. Error bars represent ±2 standard deviations based on three determinations).

Mechanical protection characteristics of the tailored nanocomposites

Studying the flexibility and adhesion properties of the fabricated and flexibility unfilled and in-situ filled silicone/single crystal γ-Al_2O_3 nanorods composite is inevitable. Impact, crosshatch and mandrel bending were investigated and their values were compared with different nanofiller loadings. Impact test results indicated the absence of any cracks in the tailored PDMS/γ-Al_2O_3 nanocomposites after testing at 100 cm/s. This result reflected excellent flexible nature and high mechanical strength (Table 1). Also no visible adhesion defects were recorded in cross-hatch test (Table 1) for any of the tested specimens which reflected the high adhesion strength. Moreover, mandrel bending investigations of the designed PDMS/γ-Al_2O_3 nanorods composite tests illustrated no visible cracking (Table 1). No intrusion was identified under a magnifying glass in any of the tested samples after penetration and bending on a < 5mm cylindrical spindle. Impact, crosshatch and bending test results reflected the high ductility and fracture resistance obtained by the as-synthesized nanocomposites.

Table 1: Mechanical tests of unfilled and single crystal γ-Al_2O_3 nanorods filled silicone nanocomposite coatings

Characteristics	**Concentration of γ-Al_2O_3 nanorods in the as-synthesized PDMS composites films**						
	0.0%	**0.05%**	**0.10%**	**0.30%**	**0.5%**	**0.7%**	**1.0%**
Impact resistance (joule)	5	9	10	15	15	10	10
Cross-hatch	Pass	Pass	Pass	Pass	Pass	Pass	Pass
T-bending	< 5	< 5	< 5	< 5	< 5	< 5	> 5

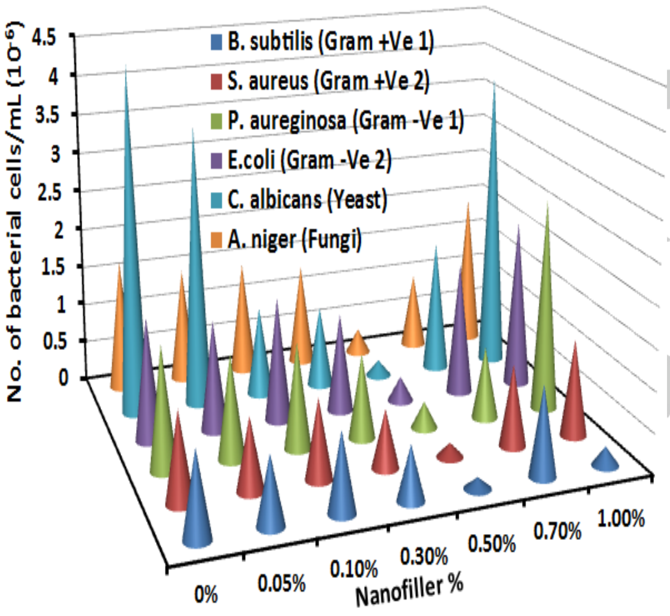

Figure 9: represent total means of bacterial counts (cells/ml) in biofilms of the tested unfilled and filled virgin and polymer/ γ-Al_2O_3 nanorod composite coatings on different bacterial, yeast and fungi strains after 28 days of incubation in broth media under light conditions.

FR efficacy investigation via biological essay

Many clumps of settled film were observed for the control sample. The biofilm suspensions that collected from the unfilled and filled PDMS/ γ-Al_2O_3 nanorods composite slides after 4 weeks of incubation were further studied for the visualization of viable bacteria (Figure 9). Cell viability measurements indicated that the presence of well-dispersed γ-Al_2O_3 nanorods in PDMS polymer (up to 0.5%) cause sharp decrease in the number of microorganisms strains which reflect the high growth inhibition. This is the result of lotus effect and homogeneous topology of the γ-Al_2O_3 nanorods which resist fouling attachments. The number of viable cells in the biofilm specimens on the polymer nanocomposite hybrid coatings (0.5%) was significantly low compared to the unfilled cured polymer surface and control (respectively). These results go in agreement with the determinations obtained from studying the surface chemistry (WCA, SFE and RMS) that reflected the high lotus-like self-cleaning features and high fouling repellency. Thus, well-dispersion of γ-Al_2O_3 nanorods into PDMS for FR coating application represents a promising strategy to inhibit the development of maritime microorganisms on the immersed surfaces via physical antiadhesion mechanism.

POM was applied to study the biofilm coverage and the ability of fouling settlements on the modeled nanocomposite surface (Figure 10). Well-dispersed nanorods especially at (0.5% γ-Al_2O_3 nanorods) promoted topological homogeneity, improved self-cleaning and surface immunity against fouling attachments. Higher γ-Al_2O_3 nanorods resulted in topological unhomogeniety, reduced self-cleaning and increased fouling settlements as a consequence of nanofiller clustering. The results from POM images approved the surface homogeneity and immunity against fouling for γ-Al_2O_3 nanorod fillers loading up to 0.5%. On contrary, at higher nano-filler loadings (up to 5%), surface topological unhomogeneity and lower self-cleaning was observed because of the nanofiller clustering that reduce the surface area of NPs and thus the matrix-NPs bonding strength.

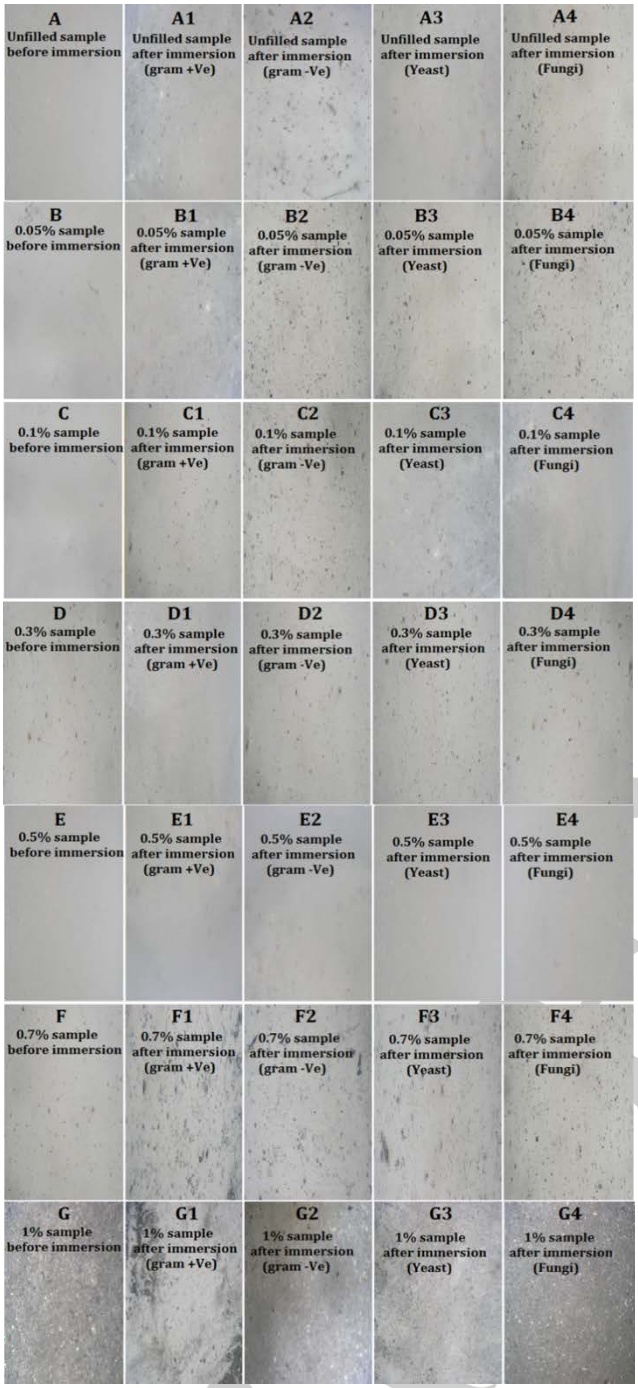

Figure 10: POM captures where (A), (A1), (A2) and (A3) of the virgin high MW PDMS; (B), (B1), (B2) and (B3) of the as-synthesized PDMS/single crystal Y-Al_2O_3 nanorods composites (with 0.05% nanofiller loadings); (C), (C1), (C2) and (C3) are the images of the PDMS/single crystal Y-Al2O3 nanorods composites (with 0.1% nanofiller loadings); (D), (D1), (D2) and (D3) corresponding to the as-synthesized PDMS/single crystal Y-Al_2O_3 nanorods composites (with 0.3% nanofiller loadings); (E), (E1), (E2) and (E3) of the prepared PDMS/single crystal Y-Al_2O_3 nanorods composites (with 0.5% nanofiller loadings); (F), (F1), (F2) and (F2) of the as-synthesized PDMS/single crystal Y-Al_2O_3 nanorods composites (with 0.7 % nanofiller loadings) and (G), (G1), (G2) and (G3) of the PDMS/ single crystal Y-Al_2O_3 nanorods composites (with 1% nanofiller loadings); all before and after immersion in gram (+Ve and –Ve) bacteria, Yeast and fungi organisms for one month.

Conclusions

This work introduces novel, ecological and economic solution for fouling problem in maritime ecosystem and shipping industry. Novel In-situ high MW PDMS/single crystal γ-Al_2O_3 nanorod composites were employed for the first time for lotus-like and self-cleaning FR coatings. Single crystal γ-Al_2O_3 nanorods were easily synthesized and controlled in shape and morphology. The lotus-like FR performance of the fabricated nanocomposites based on establishing non-leachant, nonstick, superhydrophobic self-cleaning and self-repelling paint surface. Characterization techniques of γ-Al_2O_3 approved the preparation of well-dispersed nanorods with single crystal structure, 20 nm average diameters and bounded by {400} lattice plane. High lotus-like superhydrophobic, self-cleaning and surface inertness can afford superior FR characteristics for the tailored well dispersed PDMS/single crystal γ-Al_2O_3 nanorods composites. Different concentrations of γ-Al_2O_3 nanofillers were employed and investigated for comparable studies. Investigating the surface behaviour of the newly developed virgin polymer and nanocomposites was carried out based on CA, SFE and AFM determinations. The outcomes confirmed that insertion of 0.5% γ-Al_2O_3 nanorods fillers is the most prominent because of the well-distribution of nanofillers in the polymer matrix. Well distribution of nanorods can exhibit rough topological homogeneity, maximum CA and self-cleaning property and minimum SFE and fouling cohesion. By contrast, higher nanofiller concentrations up to 0.1%, result in reduced CA, topological homogeneity and water repellency because of nanorods' agglomerations and condensation over each other's that enabled fouling settlements. No significant change in the viscoelastic properties was observed at low nanofiller percentages (0.5%). The FR performance of the fabricated nanocomposite coatings was investigated via biological assay in laboratory. The newly developed in-situ silicone/ γ-Al_2O_3 nanorods composites could possess several merits, such as cost-saving and ecological impacts, longitivity and durability that are beneficial to maritime eco-systems.

Supporting Information Summary

Supporting information contains the expermental details, including the prepration and crosslinking methods of Y-Al_2O_3 nanorods filled silicone nanocomposites, testing apparatus, surface and biological assessments as well as the results of FTIR, thermal stability and texture properties.

Keywords: Bacterial progenies; Environmentally friendly; Fouling release; lotus-like; nanocomposites.

[1] T. Hanemann, D. V. Szabo, *Materials*. **2010**; *3(6)*, 3468–517.

[2] W. J. Yang, K-G. Neoh, E-T. Kang, SL-M. Teo, D. Rittschof, *Prog Polym Sci.* **2014**; *39*, 1017-1042.

[3] R. Ciriminna, F.V. Bright, M. Pagliaro, *ACS Sustainable Chem Eng.* **2015**; *3(4)*, 559–565.

[4] S. Krishnn, C. J. Weinman, C. K. Ober, *J Mater Chem.* **2008**; *18*, 3405-3413.

[5] (a) M. S. Selim, M. A. Shenashen, S. A. El-Safty, M. Sakai, S. A. Higazy, M. M. Selim, H. Isago, A. Elmarakbi, *Prog. Mater. Sci.* **2017**; *87*, 1-32; (b) M. S. Selim, M.A. Shenashen, S. Hasegawa, N. A. Fatthallah, A. Elmarakbi, S. A. El-Safty, *Chem. Engin. J.* **2017**; *320*, 653-666.

[6] (a) M. P. Schultz, *Biofoul*. **2007**; *23*, 331–41; (b) B. Yameen, A. Farrukh, *Chem. Asian. J.* **2013**; *8(8)*, 1736–1753.

[7] IMO. International convention on the control of harmful antifouling systems on ships, International Maritime Organization, London (**2001&2008**).

[8] M. S. Selim, S. A. El-Safty, M. A. El-Sockary, A. I. Hashem, O. M. Abo Elenien, A. M. EL-Saeed, N. A. Fatthallah, *RSC Adv.* **2015**; *5(26)*, 19933–19943.

[9] M. Lejars, A. Margaillan, C. Bressy, *Chem. Rev.* **2012**; *112(8)*, 4347–4390.

[10] M. R. Detty, R. Ciriminna, F.V. Bright, M. Pagliaro, *Acc Chem Res.* **2014**; *47 (2)*, 678–687.

[11] (a) G. G. Sankar, S. Sathya, P. S. Murthy, A. Das, R. Pandiyan, V. B. Venugopalan, M. Doble. *Inter Biodetor & biodegrad.* **2015**; *104*, 307-314; (b) A. Kottmann, E. Mejía, T. Hémery, J. Klein, U. Kragl, Chem. Asian. J. **2017**; *12 (11)*, 1168-1179.

[12] K. J. Wynne, G. W. Swain, R.B. Fox, S. Bullock, J. Uilk, *Biofoul*. **2000**; *16*, 277–288.

[13] J. Y. Lin, Y. Cai, X. F. Wang, B. Ding, J. Y. Yu, M. R. Wang, *Nanoscale*. **2011**; *3*, 1258–1262.

[14] (a) R. Nishimura, K. Hyodo, H. Sawaguchi, Y. Yamamoto, Y. Nonomura, H. Mayama, S. Yokojima, S. Nakamura, K. Uchida, *J. Am. Chem. Soc.* **2016**; *138 (32),* 10299–10303; (b) L. Heng, X. Wang, Y. Dong, J. Zhai, B. Z. Tang, T. Wei, L. Jiang, *Chem. Asian. J.* **2008**; *3*, 1041-1045.

[15] M.S. Selim, S.A. El-Safty, M. A. El-Sockary, A. I. Hashem, O. M. Abo Elenien, A. M. EL-Saeed, N. A. Fatthallah, *RSC Adv.* **2015**; *5(78)*, 63175-63185.

[16] M. S. Selim, S. A. El-Safty, M. A. El-Sockary, A. I. Hashem, O. M. Abo Elenien, A. M. EL-Saeed, N. F. Fatthallah, *Mater. Design.* **2016**; *101*, 218-225.

[17] (a) Y. Lvov, E. Abdullayev, *Prog Polym Sci.* **2013**; *38*, 1690-1719; (b) Z. W. Seh, S. Liu, M-Y. Han, *Chem. Asian. J.* **2012**; *7(10)*, 2174–2184.

[18] J. Yuan, A. H. E. Müller. *Polym*. **2010**; *51(18)*, 4015–4036.

[19] S. Mallakpour, E. Khadema, *Prog Polym Sci.* **2015**; *51*, 74–93.

[20] B. Kasprzyk-Hordern, *Adv Colloid Interface Sci.* **2004**; *110*, 19–48.

[21] X. Y. Chen, H. S. Huh, S. W. Lee, *Nanotechnol*. **2007**; *18*, 285608.

[22] X. Xiao, G. Cao, F. Chen, Y. Tang, X. X. Liu, W. Xu, *Appl. Surf. Sci.* **2015**; *349*, 876-879.

[23] M. T. Khorasani, H. Mirzadeh, Z. Kermani, *Appl. Surf. Sci.* **2005**; *242(2–3)*, 339–45

[24] (a) S. Kango, S. Kalia, A. Celli, J. Njuguna, Y. Habibi, R. Kumar, *Prog Polym Sci.* **2013**; *38*, 1232–1261 (b) S. V. N. T. Kuchibhatla, A. S. Karakoti, D. Bera, S. Seal, *Prog Mater Sci.* **2007**; *52*, 699–913.

[25] A. Taguet, P. Cassagnau, J-M. Lopez-Cuesta, *Prog Polym Sci.* **2014**; *39(8),*1526-1563.

[26] (a) A. L. KOCH, *Biochim. Biophys. Acta.* **1961**; *51*, 429-441; (b) A. L. KOCH, *Anal. Biochem.* **1970**; *38*, 252-259. (Repeated in Ref. 52)

[27] B. Sun, Z. Ji, Y-P. Liao, M. Wang, X. Wang, J. Dong, C. H. Chang, R. Li, H. Zhang, A. Nel, T. Xia, *ACS NANO*. **2013**; *7(12),* 10834-10849.

[28] H. W. Hou, Y. Xie, Q. Yang, Q. X. Guo, C. R. Tan, *Nanotechnol*. **2005**; *16*, 741–745.

[39] A. S. Jbara, Z. Othaman, A. A. Ati, M. A. Saeed. *Mater. Chem. Phys.* **2017**; *188*, 24-29.

[30] A. Razmjoua, J. Mansouri, V. Chen, *J. Membr. Sci.* **2011**; *378*, 73–84.

[31] H. Datta, N. K. Singha, A.K. Bhowmick, *J Appl Polym Sci* **2008**; *108*, 2398-407.

[32] L. Feng, H. Zhang, P. Mao, Y. Wang, Y. Ge, *Appl. Surf. Sci.* **2011**; 257, 3959–3963.

[33] E. Richard, S.T. Aruna, B.J. Basu, *App. Surf. Sci.* **2012**; 258, 10199–10204.

[34] S-Y Li, J. Wang, Y. Li, C-W Wang, *Microelec. Engin.* **2015**; 142, 70–76.

[35] N. Roy, A.K. Bhowmick, *Polymer*. **2010**; *51*, 5172-5185.

[36] G. Momen, M. Farzaneh, *Appl. Surf. Sci*. **2012**; *258(15),* 5723-5728

[37] A. A. Al-Juhni, B. Z. Newby, *Prog. Org. Coat.* **2006**; *56*, 135–145.

[38] M. S. Selim, S. A. El-Sockary, M. A. El-Sockary, A. I. Hashem, O.M. Abo Elenien, A. M. EL-Saeed, N. A. Fatthallah, *Data in Brief.* **2016**; *8*, 1357-1364.

WILEY-VCH

TOC: A newly developed series of silicone/single crystal ϒ–Al_2O_3 nanorods composites was introduced via in-situ technique for marine fouling release coatings. Lotus-like self-cleaning model was introduced by the combination of both hierarchical structures and low surface free energy. Anti-bactericidal behaviour was dramatically assessed by using various microfoulants organisms. The modeled nano-system could be potentially applied in marine FR coatings via failure adhesion mechanism.

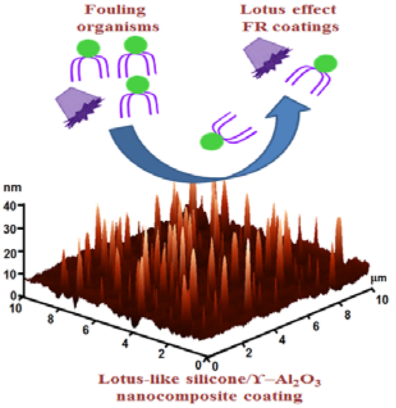

Mohamed S. Selim,[a,b] Mohamed A. Shenashen,[a, b] Nesreen A. Fatthallah,[c] Ahmed Elmarakbi [d] and Sherif A. El-Safty,[a,e,*]

Page 1 – Page 11

Title: In Situ Fabrication of One-Dimensional-Based Lotus-like Silicone/ϒ–Al_2O_3 Nanocomposites for Marine Fouling Release Coatings

WILEY-VCH